Journal of Solid State Chemistry **156**, 161–167 (2001)
doi:10.1006/jssc.2000.8977, available online at http://www.idealibrary.com on IDEAL®

A New Oxyborate in the Ternary Phase Diagrams $Li_2O–Ln_2O_3–B_2O_3$: $Li_2Ln_5O_4(BO_3)_3$ (Ln=Yb, Lu): Crystal Structure of the Ytterbium Phase

Veronique Jubera, Pierre Gravereau,[1] Jean-Pierre Chaminade, and Claude Fouassier

Institut de Chimie de la Matière Condensée de Bordeaux (ICMCB-CNRS) [UPR 9048], Université Bordeaux I, 87 Avenue du Dr Albert Schweitzer, 33608 Pessac Cedex, France

Received May 31, 2000; in revised form July 31, 2000; accepted October 3, 2000; published online December 21, 2000

A new type of lithium rare earth oxyborate of formula $Li_2Ln_5O_4(BO_3)_3$ (Ln = Yb, Lu) has been discovered in the ternary phase diagrams $Li_2O–Ln_2O_3–B_2O_3$. Single crystals of $Li_2Yb_5O_4(BO_3)_3$ were grown by the flux method. The structure of this oxyborate was solved from a data collection with a four circle automatic diffractometer and with Mo*K*α radiation. The cell is monoclinic (space group $P2_1/m$, $Z = 2$) with $a = 10.095(2)$ Å, $b = 3.519(2)$ Å, $c = 15.647(11)$ Å, $\beta = 105.45(3)°$, $V = 535.7(5)$ Å^{-3}. Refinement of 86 parameters using 3298 independent reflections having intensity $I > 2\sigma(I)$ led to $R = 0.037$ (w$R = 0.091$). The structure of $Li_2Yb_5O_4(BO_3)_3$ is made up of a bidimensional framework of edge or corner-sharing YbO_7 polyhedra parallel to the $(10\bar{1})$ plane and connected by three-coordinated boron atoms and lithium ions. It can also be described as a bidimensional assembly of OYb_4 tetrahedra, $((Yb_{10}O_8)^{14+})_n$, separated by borate groups and lithium coordination polyhedra forming ribbons, $((Li_4B_6O_{18})^{14-})_n$, along the b direction. The presence of oxygen atoms sharing only Yb polyhedra justifies the oxyborate label. © 2001 Academic Press

Key Words: **crystal structure; oxyborate of lithium and ytterbium; rare earth compounds.**

INTRODUCTION

An investigation of the Gd_2O_3-rich part of the $Li_2O–Gd_2O_3–B_2O_3$ ternary phase diagram recently led us to discover a new composition $LiGd_6B_3O_{14}$ whose structure has been solved. A family of isostructural phases $LiLn_6O_5(BO_3)_3$ has been obtained for Ln = Pr–Tm (1). For the heavy rare earths such as Yb and Lu, this phase does not exist. Nevertheless in the vicinity of the $LiLn_6O_5(BO_3)_3$ composition appears the new phase $Li_2Ln_5O_4(BO_3)_3$ which has been first characterized by its X-ray diffraction powder pattern. Then, the growth of single crystals for Ln = Yb has permitted the crystal structure determination of this new type of borate.

PREPARATION PROCESS

Powder Preparation

Polycrystalline samples were prepared using stœchiometric mixture of reagent grade starting materials following the reaction

$$\tfrac{5}{2}Ln_2O_3 + 3H_3BO_3 + 2LiOH{,}H_2O$$
$$\rightarrow Li_2Ln_5O_4(BO_3)_3 + \tfrac{15}{2}H_2O\uparrow$$

The thermal process consists of two steps: first preheating at 700°C for 3 h, and then, after grinding, sintering at 900°C for 15 h under air atmosphere. The final products were controlled by X-ray powder diffraction analysis using Cu*K*α radiation.

Crystal Growth

Single crystals have been grown by the flux method in the Li–Yb–B–O system as $Li_2Yb_5O_4(BO_3)_3$ does not melt congruently. Different compositions in the ternary phase diagram were investigated. They were heated to 1200°C for 6 h and then slowly cooled at 2°C/h to 900°C and finally at 50°C/h to room temperature. Single crystals were selected by optical examination in the partially melted mixture. Crystals grew as transparent colorless needles.

STRUCTURAL DETERMINATION OF $Li_2Yb_5O_4(BO_3)_3$

Weissenberg and Burger photographs indicated that the compound belongs to the monoclinic system with $P2_1/m$ and $P2_1$ as possible space groups ((0k0), $k = 2n$). Data collection with a CAD4 Enraf Nonius automatic diffractometer using the Mo*K*α radiation covered half the reciprocal space (6304 reflections with $I > 2\sigma(I)$) up to $\theta = 40°$. The unit cell parameters were refined from 25 reflections in the range of $1° < \theta < 23°$. The crystal data and experimental conditions are listed in Table 1. The data were corrected for

---

[1] To whom correspondence should be addressed. Fax: + 33(0)5 56 84 27 61. E-mail: graver@icmcb.u-bordeaux.fr.

0022-4596/01 $35.00

TABLE 1
Crystal data and structure refinement for $Li_2Yb_5O_4(BO_3)_3$

Crystal data	
Empirical formula	$Li_2Yb_5O_4(BO_3)_3$
Formula weight	1119.5 g
Crystal system	Monoclinic
Space group	$P2_1/m$
Unit cell dimensions	$a = 10.095(2)$ Å $b = 3.519(2)$ Å $c = 15.647(11)$ Å $\beta = 105.45(3)$ (°)
Volume	535.7(5) Å^3
Z	2
F(000)	916
Temperature	293(2) K
ρ_{cal}	6.93 Mg/m^3
Absorption coefficient	43.2 mm^{-1}
Crystal shape	Needle
Crystal colour	White
Crystal size	0.100 × 0.050 × 0.180 mm
Data collection	
Diffractometer	Enraf-Nonius CAD4
Radiation	Mo$K\alpha$ ($\lambda = 0.71073$ Å)
Monochromator	Graphite
θ Range	1–40 (°).
Index ranges	$-18 \le h \le 18$ $0 \le k \le 6$ $-28 \le l \le 28$
Scan type	ω/θ
Scan width	$1.15 + 0.35 \tan\theta$ (°)
Reflections collected ($I > 2\sigma(I)$)	6304
Indep. reflections ($I > 2\sigma(I)$)	3298 ($R_{int} = 0.036$)
Refinement	
Absorption correction	Psi-scan
Max. and min. transmission	0.116 and 0.050
Refinement method	Full-matrix L.S. on F^2
Data / parameters refined	3298/86
Weighting scheme	$\omega = 1/[\sigma^2(Fo^2) + (0.0351P)^2 + 18.04P]$ where $P = (Fo^2 + 2Fc^2)/3$
Extinction coefficient	0.0067(3)
Goodness-of-fit on F^2	1.19
Final R indices ($I > 2\sigma(I)$)	$R_1 = 0.037$, w$R_2 = 0.091$
Max. shift/esd	< 0.001
Largest diff. peak and hole	4.91 and −5.48 e Å^{-3}

TABLE 2
Atomic Coordinates and Equivalent Isotropic (isotropic for B, Li, and O) Displacement Parameters (Å^2) for $Li_2Yb_5O_4(BO_3)_3$

Atom	Site	x	y	z	U_{eq}/U^*_{iso}
Li(1)	2e	0.614(2)	0.25	0.053(2)	0.015(4)*
Li(2)	2e	0.246(4)	0.25	0.752(2)	0.034(4)*
Yb(1)	2e	0.0351(1)	0.25	0.3731(1)	0.0052(1)
Yb(2)	2e	0.5195(1)	0.25	0.3018(1)	0.0035(1)
Yb(3)	2e	0.1449(1)	0.25	0.9992(1)	0.0029(1)
Yb(4)	2e	0.6400(1)	0.25	0.5626(1)	0.0024(1)
Yb(5)	2e	0.8134(1)	0.25	0.7941(1)	0.0025(1)
B(1)	2e	0.4100(11)	0.25	0.1104(7)	0.0077(14)*
B(2)	2e	0.2144(10)	0.25	0.5760(6)	0.0054(13)*
B(3)	2e	0.9061(10)	0.25	0.1824(6)	0.0058(13)*
O(1)	2e	0.3798(7)	0.25	0.0195(4)	0.0075(10)*
O(2)	2e	0.2972(7)	0.25	0.1489(4)	0.0065(9)*
O(3)	2e	0.5417(9)	0.25	0.1634(6)	0.0168(14)*
O(4)	2e	0.0803(7)	0.25	0.5837(5)	0.0081(10)*
O(5)	2e	0.2365(7)	0.25	0.4930(5)	0.0075(10)*
O(6)	2e	0.3221(7)	0.25	0.6528(4)	0.0065(9)*
O(7)	2e	0.8298(7)	0.25	0.0959(5)	0.0087(10)*
O(8)	2e	0.8465(8)	0.25	0.2527(5)	0.0106(11)*
O(9)	2e	0.0488(7)	0.25	0.2065(4)	0.0065(9)*
O(10)	2e	0.4877(6)	0.25	0.4317(4)	0.0037(8)*
O(11)	2e	0.6116(6)	0.25	0.7042(4)	0.0046(9)*
O(12)	2e	0.8519(6)	0.25	0.6541(4)	0.0046(9)*
O(13)	2e	0.9178(6)	0.25	0.9376(4)	0.0040(8)*

Note. U(eq) is defined as one-third of the trace of the orthogonalized U_{ij} tensor.

Lorentz-polarization effects and empirical absorption corrections were carried out using psi-scans on 8 reflections in the range $6° < \theta < 27°$, leading to 3298 unique reflections ($Fo^2 > 2\sigma(Fo^2)$) with a R_{int} index of 0.036.

The structure was solved by Patterson function deconvolution and heavy atoms method in $P2_1/m$ space group. Five sites of ytterbium atoms were located (SHELXS86) (2). The positions of oxygen, boron and lithium atoms were given by refinement and successive Fourier difference functions (SHELXL93) (3) (Table 2). The refinement with anisotropic (Yb) and isotropic (Li, B, O) displacement parameters and secondary extinction factor converged to $R_1 = 0.037$ (w$R_2 = 0.091$). Anisotropic atomic displacement parameters were not refined for oxygen, lithium, and boron because the obtained values seemed us to be artifact results and the improvement on R_1 and wR_2 was not significant enough to be considered (Table 2, 3). Selected interatomic distances and angles are listed in Table 4. Residual density maxima are found near the ytterbium atoms with distances ranging from 0.45 to 1.15 Å; they were located along the Yb–O bonds. This has been already observed in other structural determinations of rare earth compound ($LiLn_6O_5(BO_3)_3$, Ln from Pr to Tm (1)). It may be due to

TABLE 3
Anisotropic Displacement Parameters (Å^2) for $Li_2Yb_5O_4(BO_3)_3$

	U_{11}	U_{22}	U_{33}	U_{23}	U_{13}	U_{12}
Yb(1)	0.0027(1)	0.0027(1)	0.0108(1)	0.0000	0.0030(1)	0.0000
Yb(2)	0.0044(1)	0.0025(1)	0.0045(1)	0.0000	0.0029(1)	0.0000
Yb(3)	0.0024(1)	0.0023(1)	0.0045(1)	0.0000	0.0016(1)	0.0000
Yb(4)	0.0019(1)	0.0022(1)	0.0033(1)	0.0000	0.0009(1)	0.0000
Yb(5)	0.0019(1)	0.0025(1)	0.0032(1)	0.0000	0.0010(1)	0.0000

Note. The anisotropic displacement factor exponent takes the form $-2\pi^2(h^2a^{*2}U_{11} + \cdots + 2hka^*b^*U_{12} + \cdots)$.

TABLE 4
Selected Bond Lengths [Å] and Angles [°] for $Li_2Yb_5O_4(BO_3)_3$

B(1)–O(3)	1.367(14)	B(2)–O(5)	1.374(12)	B(3)–O(7)	1.367(13)
B(1)–O(1)	1.373(13)	B(2)–O(6)	1.390(12)	B(3)–O(8)	1.387(13)
B(1)–O(2)	1.423(13)	B(2)–O(4)	1.391(12)	B(3)–O(9)	1.388(12)
⟨B(1)–O⟩	1.387	⟨B(2)–O⟩	1.385	⟨B(3)–O⟩	1.380
O(1)–B(1)–O(2)	117.2(8)	O(4)–B(2)–O(6)	118.6(8)	O(8)–B(3)–O(9)	114.9(8)
O(2)–B(1)–O(3)	120.1(9)	O(4)–B(2)–O(5)	119.3(8)	O(7)–B(3)–O(8)	122.4(8)
O(1)–B(1)–O(3)	122.6(9)	O(5)–B(2)–O(6)	122.1(8)	O(7)–B(3)–O(9)	122.6(8)
⟨O–B(1)–O⟩	119.9	⟨O–B(2)–O⟩	120.0	⟨O–B(3)–O⟩	119.9

Li(1)–O(3)	2.04(3)	Li(1)–B(1)	2.45(3)	Li(2)–O(6)	1.90(4)	Li(2)–B(2)	2.68(4)
Li(1)–O(1)^{2}	2.107(14)			Li(2)–O(8)^{4}	1.98(2)	Li(2)–B(3)^{4}	2.71(3)
Li(1)–O(1)^{3}	2.107(14)			Li(2)–O(8)^{5}	1.98(2)	Li(2)–B(3)^{5}	2.71(3)
Li(1)–O(7)	2.11(3)			Li(2)–O(4)	2.71(4)		
Li(1)–O(1)	2.28(3)			Li(2)–O(3)^{4}	2.82(3)		
⟨Li(1)–O⟩	2.128			Li(2)–O(3)^{5}	2.82(3)		
				⟨Li(2)–O⟩	2.370		

Yb(1)–O(12)^{5}	2.200(4)	Yb(2)–O(10)	2.140(6)	Yb(3)–O(13)^{13}	2.192(4)
Yb(1)–O(12)^{4}	2.200(4)	Yb(2)–O(11)^{4}	2.190(4)	Yb(3)–O(13)^{12}	2.192(4)
Yb(1)–O(8)^{9}	2.295(8)	Yb(2)–O(11)^{5}	2.190(4)	Yb(3)–O(13)^{9}	2.238(6)
Yb(1)–O(4)^{7}	2.310(5)	Yb(2)–O(3)	2.237(10)	Yb(3)–O(1)^{1}	2.307(7)
Yb(1)–O(4)^{8}	2.310(5)	Yb(2)–O(6)^{5}	2.356(5)	Yb(3)–O(7)^{4}	2.363(5)
Yb(1)–O(5)	2.370(7)	Yb(2)–O(6)^{4}	2.356(5)	Yb(3)–O(7)^{5}	2.363(5)
Yb(1)–O(9)^{9}	2.647(7)	Yb(2)–O(2)	2.810(7)	Yb(3)–O(2)^{1}	2.435(7)
⟨Yb(1)–O⟩	2.333	⟨Yb(2)–O⟩	2.325	⟨Yb(3)–O⟩	2.299

Yb(4)–O(10)^{4}	2.199(4)	Yb(5)–O(11)	2.145(7)
Yb(4)–O(10)^{5}	2.199(4)	Yb(5)–O(13)	2.211(6)
Yb(4)–O(10)	2.210(6)	Yb(5)–O(9)^{11}	2.245(4)
Yb(4)–O(12)	2.235(7)	Yb(5)–O(9)^{10}	2.245(4)
Yb(4)–O(11)	2.309(7)	Yb(5)–O(12)	2.326(7)
Yb(4)–O(5)^{5}	2.447(5)	Yb(5)–O(2)^{4}	2.380(5)
Yb(4)–O(5)^{4}	2.447(5)	Yb(5)–O(2)^{5}	2.380(5)
⟨Yb(4)–O⟩	2.292	⟨Yb(5)–O⟩	2.276

⟨O(10)–Yb⟩	2.186	⟨O(11)–Yb⟩	2.208
Yb(2)–O(10)–Yb(4)^{4}	106.0(2)	Yb(5)–O(11)–Yb(2)^{4}	119.1(2)
Yb(2)–O(10)–Yb(4)^{5}	106.0(2)	Yb(5)–O(11)–Yb(2)^{5}	119.1(2)
Yb(2)–O(10)–Yb(4)	129.5(3)	Yb(5)–O(11)–Yb(4)	106.9(3)
Yb(4)^{4}O(10)–Yb(4)^{5}	106.4(3)	Yb(2)^{4}–O(11)–Yb(2)^{5}	107.0(3)
Yb(4)^{4}–O(10)–Yb(4)	103.5(2)	Yb(2)^{4}–O(11)–Yb(4)	100.7(2)
Yb(4)^{5}–O(10)–Yb(4)	103.5(2)	Yb(2)^{5}–O(11)–Yb(4)	100.7(2)
⟨Yb–O–Yb⟩	109.1	⟨Yb–O–Yb⟩	108.9
⟨O(12)–Yb⟩	2.240	⟨O(13)–Yb⟩	2.208
Yb(1)^{5}–O(12)–Yb(1)^{4}	106.3(3)	Yb(3)^{13}–O(13)–Yb(3)^{12}	106.8(3)
Yb(1)^{5}–O(12)–Yb(4)	109.4(2)	Yb(3)^{13}–O(13)–Yb(5)	109.8(2)
Yb(1)^{5}–O(12)–Yb(5)	114.1(2)	Yb(3)^{13}–O(13)–Yb(3)^{6}	101.1(2)
Yb(1)^{4}–O(12)–Yb(4)	109.4(2)	Yb(3)^{12}–O(13)–Yb(5)	109.8(2)
Yb(1)^{4}–O(12)–Yb(5)	114.1(2)	Yb(3)^{12}–O(13)–Yb(3)^{6}	101.1(2)
Yb(4)–O(12)–Yb(5)	103.4(3)	Yb(5)–O(13)–Yb(3)^{6}	126.4(3)
⟨Yb–O–Yb⟩	109.4	⟨Yb–O–Yb⟩	109.2

Note. Symmetry transformations used to generate equivalent atoms: 1, $x, y, z+1$; 2, $-x+1, -y, -z$; 3, $-x+1, -y+1, -z$; 4, $-x+1, -y, -z+1$; 5, $-x+1, -y+1, -z-1$; 6, $x+1, y, z$; 7, $-x, -y, -z+1$; 8, $-x, -y+1, -z+1$; 9, $x-1, y, z$; 10, $-x+2, -y, -z+1$; 11, $-x+2, -y+1, -z+1$; 12, $-x+1, -y, -z+2$; 13, $-x+1, -y+1, -z+2$.

TABLE 5
Lattice Parameters and Densities Calculated from Powder Data

	a (Å)	*b* (Å)	*c* (Å)	*β* (°)	*V* (Å^3)	Calculated densities	Experimental densities
$Li_2Yb_5O_4(BO_3)_3$	10.0974(2)	3.5248(1)	15.6530(4)	105.450(2)	536.97(3)	6.926(1)	6.96(1)
$Li_2Lu_5O_4(BO_3)_3$	10.0652(3)	3.5052(1)	15.6602(5)	105.494(2)	532.42(1)	7.046(1)	7.02(1)

systematic errors on absorption correction and also to the fact that scattering factors assimilate atoms to spheres and so ignore bonding effects on the electronic cloud orientation.

Lattice parameters refined from powder data with the Fullprof (4) program for the Yb and Lu phases are listed in Table 5. The densities calculated from cell dimensions are close to the measured values.

Then, all atom environments were controlled with valence bond sums based on bond strength analysis (5). Results reported in Table 6 are in good agreement with the formal oxidation state of Li^+, Yb^{3+}, B^{3+}, and O^{2-} ions.

Structure Description

All atoms are located on the 2e sites (x, $\frac{1}{2}$, z) of the $P2_1/m$ centric space group. Unlike the $LiLn_6O_5(BO_3)_3$ structure in which rare earth polyhedra form a three-dimensional array of *Ln* polyhedra, the new oxyborate is built by edge-or corner-sharing ytterbium polyhedra constituting layers

TABLE 6
Valence Bond Analysis of $Li_2Yb_5O_4(BO_3)_3$

	Li(1)	Li(2)	B(1)	B(2)	B(3)	Yb(1)	Yb(2)	Yb(3)	Yb(4)	Yb(5)	$\sum s$	Expected
O(1)	0.178		0.995					0.397			1.86	2
O(1)	0.178		—					—				
O(1)	0.112		—					—				
O(2)			0.869				0.102	0.281		0.326	1.90	2
O(2)			—				—	—		0.326		
O(3)	0.211	0.026	1.011				0.479				1.75	2
O(3)	—	0.026	—				—					
O(4)		0.035		0.947		0.394					1.77	2
O(4)		—		—		0.394						
O(5)				0.992		0.335			0.272		1.87	2
O(5)				—		—			0.272			
O(6)		0.308		0.950			0.348				1.95	2
O(6)		—		—			0.348					
O(7)	0.177				1.011			0.341			1.87	2
O(7)	—				—			0.341				
O(8)		0.247			0.958	0.410					1.86	2
O(8)		0.247			—	—						
O(9)					0.955	0.158				0.469	2.05	2
O(9)					—	—				0.469		
O(10)							0.623		0.534		2.21	2
O(10)							—		0.534			
O(10)							—		0.516			
O(11)							0.544		0.395	0.615	2.10	2
O(11)							0.544		—	—		
O(12)						0.530			0.482	0.377	1.92	2
O(12)						0.530			—	—		
O(13)								0.541		0.514	2.07	2
O(13)								0.541		—		
O(13)								0.478		—		
$\sum s$	0.86	0.89	2.88	2.89	2.92	2.75	2.99	2.92	3.01	3.10		
Expected	1	1	3	3	3	3	3	3	3	3		

Note. Li–O, $s = \exp[(1.466 - d_i)/0.37]$; B–O, $s = \exp[(1.37 - d_i)/0.37]$; Yb–O, $s = \exp[(1.965 - d_i)/0.37]$.

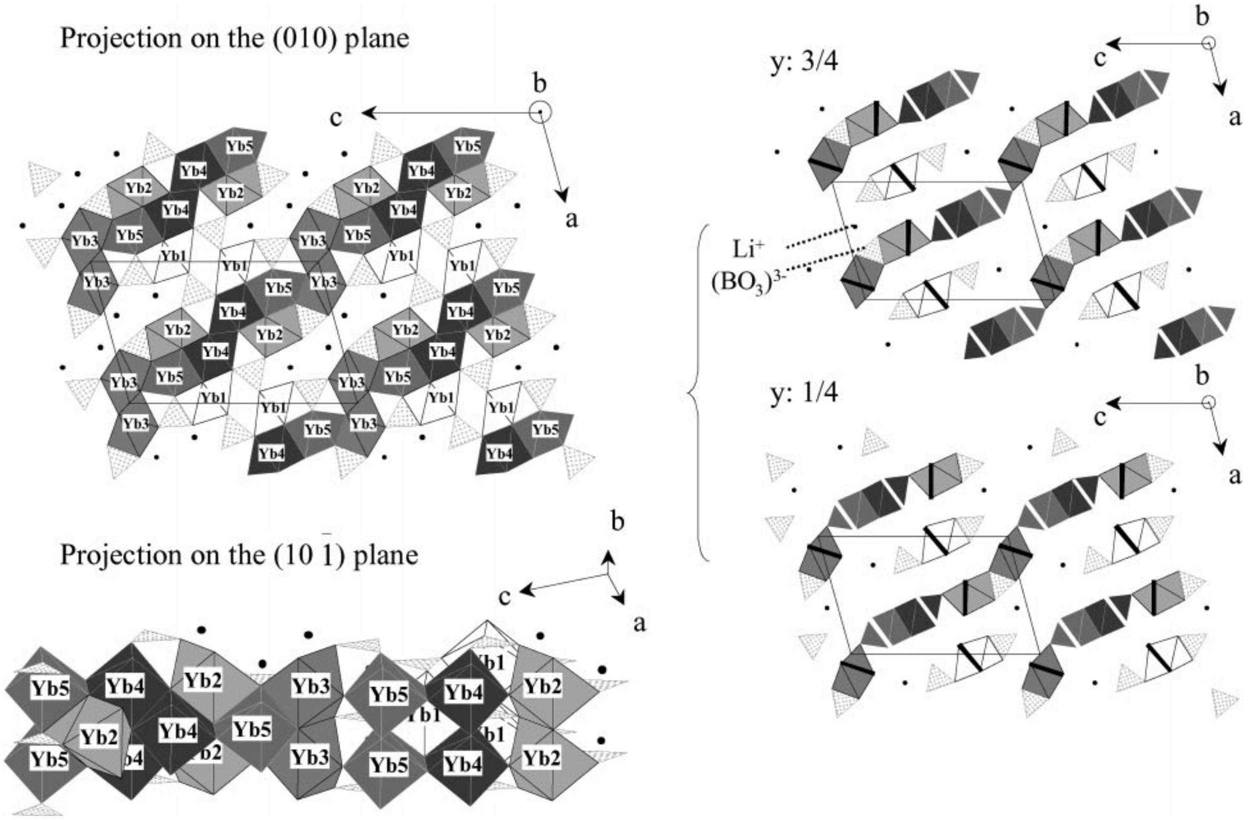

FIG. 1. Representation of the structure based on an assembly of YbO_7 polyhedra. On the right, the arrangement of Yb polyhedra centered at $y = \frac{1}{4}$ and $y = \frac{3}{4}$ has been represented. Thick lines connect oxygen atoms at the $y + 0.5$ positions.

parallel to the $(10\bar{1})$ plane. These layers are connected by isolated borate groups giving rise to a three-dimensional network whose cavities are occupied by lithium atoms (Fig. 1).

Ytterbium atom environment. The ytterbium atoms occupy five different crystallographic sites. They are coordinated with seven oxygens which form monocapped octahedra (Fig. 2). A similar environment has been encountered in yttrium borate $Y_{17.33}(BO_3)_4(B_2O_5)_2O_{16}$ (6), in the A-type rare earth sesquioxides (7) and the borates $LiLn_6O_5(BO_3)_3$ (1). Yb–O bond distances range from 2.140(6) to 2.447(5) Å with one long distance in the case of Yb(1) and Yb(2) (Yb(1)–O(9): 2.647(7) Å and Yb(2)–O(2): 2.810(7) Å). Each ytterbium polyhedron is connected by 6 (Yb(1)), 8 (Yb(2), Yb(3)), or 10 (Yb(4), Yb(5)) neighboring ytterbium polyhedra by common edges and corners (Fig. 1). Intralayer distances between ytterbium atoms range from 3.42 Å (Yb(3)–Yb(3)) to 3.73 Å (Yb(2)–Yb(5)) and interlayer distances from 4.56 Å (Yb(1)–Yb(1)) to 6.73 Å (Yb(2)–Yb(3)).

Boron atom environment. All borate groups consist of a boron triangularly coordinated to oxygen atoms. Three types of crystallographic independent isolated $(BO_3)^{3-}$ groups parallel to the (*ac*) plane are generated. The arrangement of borate groups in parallel planes is commonly observed in borate and oxyborate compounds (8). Distortions to the ideal borate group in which B–O distances and O–B–O angles are equal to about 1.38 Å and 120° respectively, are weak in this new oxyborate: B–O distances vary from 1.367 to 1.423 Å, O–B–O angles from 114.9° to 122.6°. B–O distances in structures containing isolated B triangles range in the same order of value, 1.360 to 1.399 Å in $LiGd_6O_5(BO_3)_3$ (1), 1.353 to 1.411 Å in $Li_6Y(BO_3)_3$ (9).

Borate groups are connected to ytterbium and lithium polyhedra by common edges and corners. B(1) shares corners with 2Li(1), 2Li(2), and 2Yb(5), and edges with 1Li(1), 1Yb(2), and 1Yb(3). B(2) shares corners with 3Yb(1), 2Yb(2), and 2Yb(4) and an edge with 1Li(2). B(3) shares corners with 1Li(1), 2Li(2), 2Yb(3), and 2Yb(5) and an edge with 1Yb(1) (Fig. 3).

Lithium atom environment. The unit cell contains two different types of lithium atoms. Li(1) and Li(2) are surrounded respectively by five and six oxygen atoms (Fig. 2). Li(2) has a larger environment with five $(BO_3)^{3-}$ groups: two $(B(3)O_3)^{3-}$ and one $(B(2)O_3)^{3-}$ on one side and two farther $(B(1)O_3)^{3-}$ on the other side. In the environment of

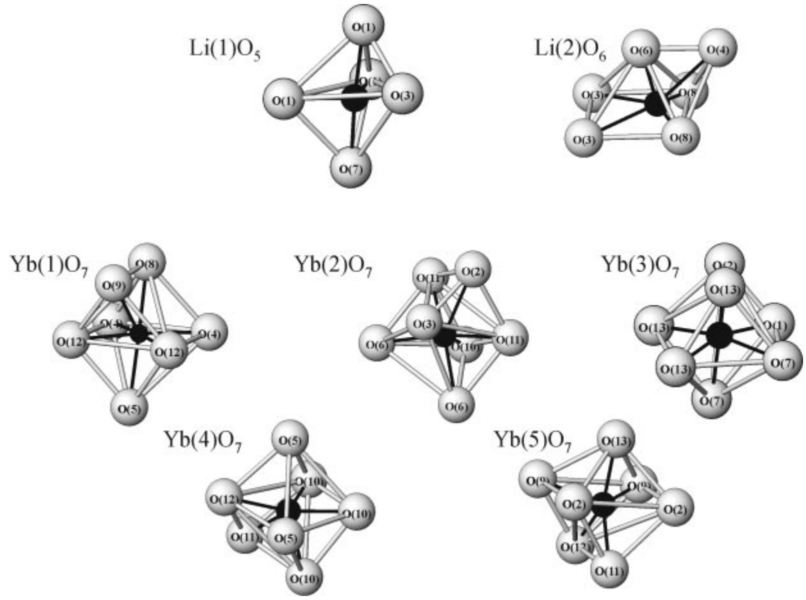

FIG. 2. Anionic polyhedra.

Li(2), three Li(2)–O distances are higher than those of Li(2)–B(2) and Li(2)–B(3). However, if these three oxygen contributions are not taken into account for the valence bond sums, the obtained values are not satisfying for the oxidation state of Li(2), O(3), and O(4) (Table 6).

The bond distances for Li(1) range from 2.040 to 2.277 Å in a nearly regular environment. The Li(1)O$_5$ polyhedra can be described as a triangular-based bipyramid whose O(1) and O(3) form the base and O(1) and O(7) constitute apices.

In the case of Li(2), the polyhedron is greatly distorted with three short distances 1.902 Å and 1.983 Å × 2 and three long distances ranging from 2.711 to 2.820 Å.

In spite of such long distances, the coordination polyhedron can be regarded as a distorted monocapped pyramid. The existence of such long distances explains the more important thermal agitation for Li(2) (Table 2).

Li(*i*) and Li(*i*) share common edges, whereas the connection between Li(*i*) and Li(*j*) is done by common corner.

Lithium polyhedra and borate groups constitute a $((Li_4B_6O_{18})^{14-})_n$ anionic group running in the *b* direction (Fig. 3). These groups are inserted between ytterbium polyhedra blocks but they are not linked each other in the [101] direction. In the case of $LiGd_6O_5(BO_3)_3$, isolated $(Li_2B_6O_{18})^{16-}$ groups are inserted in the vacant sites created by successive layers of rare earth polyhedra. As discussed for $LiGd_6O_5(BO_3)_3$, because of the weak strength of Li–O bonds, the shape of the lithium site depends strongly on the three-dimensional network of rare earth polyhedra and boron triangles.

Oxygen atom environment. Oxygen atoms can be divided into three groups depending on their cationic bonding. O(1 to 9) oxygen atoms belong to the $(BO_3)^{3-}$ groups. O(2), O(5), and O(9) are bonded to Yb^{3+} ions, O(1), O(3), O(4), O(6), O(7), and O(8) to Li^+ and Yb^{3+} ions. O(10), O(11), O(12), and O(13) oxygen atoms are only bonded to Yb atoms to constitute $(OYb_4)^{10+}$ tetrahedra. Distances and angles of these polyhedra are listed in Table 4. Because of these oxygen atoms and similarly to Li*Ln*$_6$O$_5$(BO$_3$)$_3$, the compound can be labeled oxyborate of lithium and ytterbium. Note that in all Yb coordination polyhedra these last Yb–O distances correspond to the shortest bonds (2.140–2.326 Å). Because of the highly covalent character of B–O bonds, the Yb–O bonds formed with oxygen of borate groups are weakened.

A representation of the structure based on an assembly of OYb_4 tetrahedra is given in Fig. 3. If we consider this tetrahedral arrangement, the structure can be described as a succession of $((Yb_{10}O_8)^{14+})_n$ layers parallel to the $(10\bar{1})$ plane and $((Li_4B_6O_{19})^{14-})_n$ chains parallel to the [010] direction.

CONCLUDING REMARKS

In a previous paper we reported a novel family of oxyborates of formula Li*Ln*$_6$O$_5$(BO$_3$)$_3$ (*Ln* = Pr, Nd, Sm, Eu, Gd, Tb, Dy, Ho, Er, Tm, and for Y (1)) whose the structural type was determined on a single crystal of the Gd phase. The new type of oxyborates with the composition Li$_2$*Ln*$_5$O$_4$(BO$_3$)$_3$ and whose structure has been described here has been found only for the smaller rare earth ions, Yb and Lu. The existence of two structural types in the *Ln*$_2$O$_3$-rich part of the ternary diagram may be due to a steric effect.

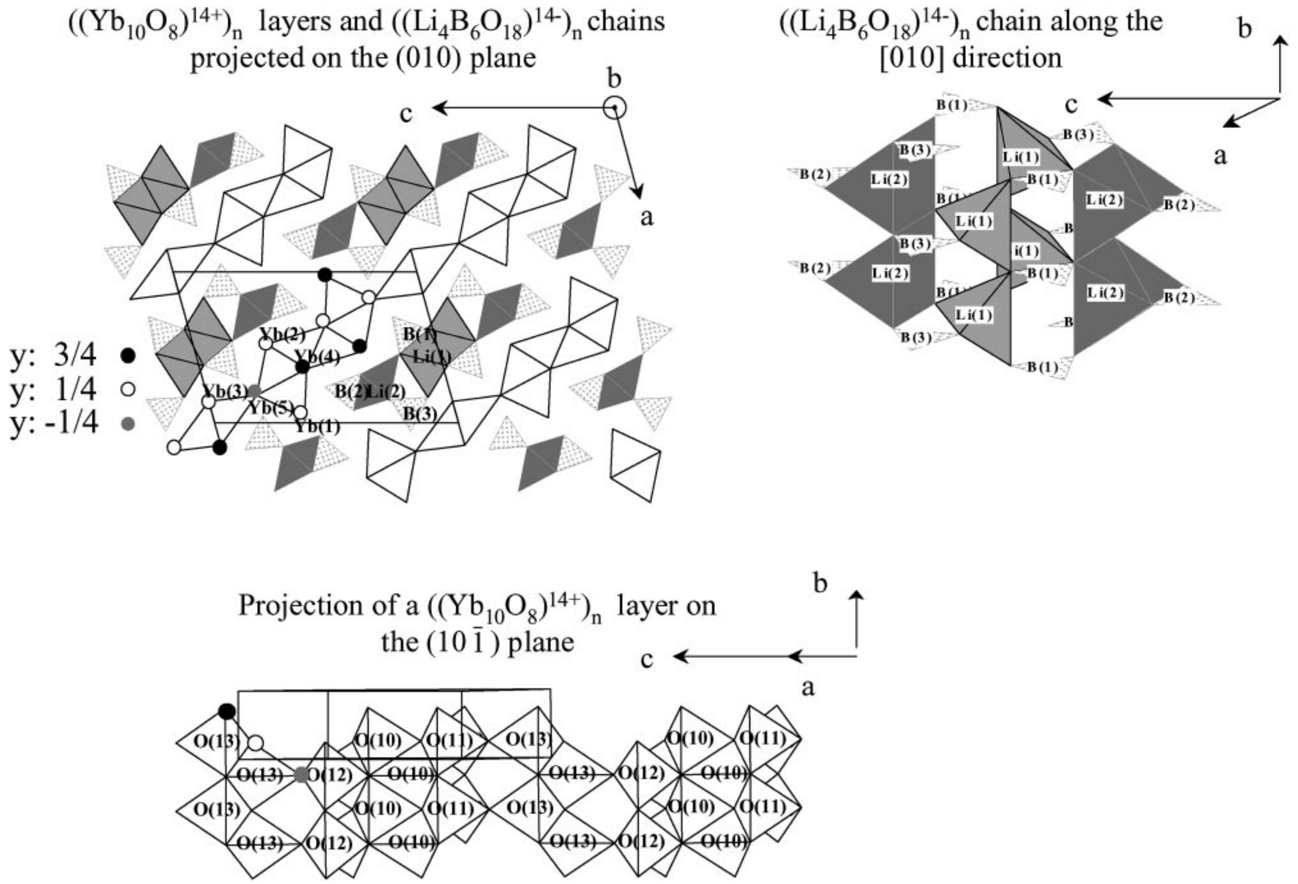

FIG. 3. Representation of the structure based on an assembly of OYb_4 polyhedra.

The structures of the two types of oxyborates differ by the dimensionality of the assembly of the rare earth coordination polyhedra.

—$LiLn_6O_5(BO_3)_3$ (*Ln* from Pr to Tm) exhibit a three-dimensional array of *Ln* polyhedra, which can be related to that of the fluorite CaF_2. *Ln–Ln* distances range from 3.62 to 3.98 Å in the (*ac*) plane and from 3.56 to 4.27 Å in the (102) plane (1).

—In $Li_2Ln_5O_4(BO_3)_3$ a new arrangement appears with independent thick layers of ytterbium polyhedra. *Ln–Ln* distances range from 3.42 to 3.73 Å (Yb(2)–Yb(5)) in a layer and from 4.56 to 6.73 Å between consecutive layers.

The structure of the two oxyborates can also be described on the basis of an assembly of OLn_4, three-dimensional in $LiLn_6O_5(BO_3)_3$ and bidimensional in $Li_2Ln_5O_4(BO_3)_3$. The $((Yb_{10}O_8)^{14+})_n$ layers encountered in the latter present strong structural relationship with the $(LnO)_n^{n+}$ layers found by Caro (10) in a large number of rare earth oxysalts. These structures are built of layers of edge-sharing OLn_4 tetrahedra which alternate with sheets of the anion groups (O^{2-} in A-Ln_2O_3, Cl^- in $LnOCl$, $(SO_4)^{2-}$ in $Ln_2O_2SO_4$, CO_3^{2-} in $Ln_2O_2CO_3$ (11)). In the $Li_2Ln_5O_4(BO_3)_3$ structure, the OLn_4 tetrahedra are linked by edges or corners in a $((Yb_{10}O_8)^{14+})_n$ tilted layer. The more complex anion group $((Li_4B_6O_{18})^{14-})_n$ constitutes ribbons parallel to the *b* direction.

Luminescence properties of Ce^{3+} and Eu^{3+} in this matrix will be the subject of future papers.

REFERENCES

1. J. P. Chaminade, P. Gravereau, V. Jubera, and C. Fouassier, *J. Solid State Chem.* **146,** 189 (1999).
2. G. M. Sheldrick, "SHELXS86: A Program for the Solution of the Crystal Structures." Univ. of Göttingen, 1986.
3. G. M. Sheldrick, "SHELXL93: A Program for Crystal Structure Refinement." Univ. of Göttingen, 1993.
4. J. Rodriguez-Carvajal, "Fullprof: A Program for Rietveld Refinement and Pattern Matching Analysis," Collected Abstract of Powder Diffraction Meeting, Toulouse, France, Vol. 127, 1990.
5. L. D. Brown and D. Altermatt, *Acta Crystallogr.* **41,** 244 (1985).
6. J. H. Lin, S. Zhou, L. Q Yang, G. Q. Yao, and M. Z. Su, *J. Solid State Chem.* **134,** 158 (1997).
7. O. Greis, *J. Solid State Chem.* **34,** 39 (1980).
8. P. Becker, *Adv. Mater.* **10,** 979 (1998).
9. T. Chao-Yuang, J. Ai-Dong, and L. Zun-Du, *J. Struct. Chem.* **8,** 215 (1989).
10. P. E. Caro, *J. Less-Common Metals* **I6,** 367 (1968).
11. J. P. Attfield and G. Férey, *J. Solid State Chem.* **82,** 132 (1989).